of rather generalized, small (20–70 cm in length) fishes, with dentitions lacking anterior fangs, a morphological category represented in the analysis by *Kenichthys*, *Gogonasus*, *Osteolepis* (Fig. 4a), *Medoevia*, the canowindrids and *Tristichopterus* (Fig. 4b). Rhizodonts[26], derived tristichopterids[27] and elpistostegids+ tetrapods[5,16,28], in contrast, show parallel trends towards a quite different morphology: they increased dramatically in size, reduced or lost their median fins, acquired diphycercal tails with a low aspect ratio, and developed a pair of fangs at the lower jaw symphysis (Fig. 4c–e). Rhizodonts and derived tristichopterids also acquired premaxillary fangs[27,29]. Rhizodonts seem to have retained a primitive, short-snouted skull morphology (J. Jeffery, personal communication). However, tristichopterids and elpistostegids+tetrapods, having a moderately lengthened snout as a synapomorphy (Fig. 4b), independently developed this character further in parallel (Fig. 4d, e). Derived tristichopterids such as *Mandageria*[29] (Fig. 4d) have very elpistostegid-like head proportions.

These changes seem to have occurred during the Middle/Late Devonian period in all three groups. Elpistostegids originated in the latest Givetian[6]; the earliest known derived tristichopterid is the Frasnian *Platycephalichthys*[23,27]; and the earliest known large rhizodont is the Famennian *Sauripteris*[15].

Our analysis indicates that much of the lower part of the tetrapodomorph stem lineage consisted of 'osteolepiform' fishes. The character attributes of this part of the stem lineage can be reconstructed with precision. Parallel evolution towards the morphology of a large predator, with reduced median fins and elaborate anterior dentition, occurred at about the same time in rhizodonts, tristichopterids, and elpistostegids+tetrapods (Fig. 4). The evolution of two latter clades, having extra synapomorphies, also paralleled each other more closely. The Tetrapoda thus arose out of one of several similar evolutionary 'experiments' with a large aquatic predator role. Closer study of these parallel radiations should cast much new light on the ecological background to the origin of tetrapods. □

Methods

Phylogenetic analysis. The analysis was performed using the software package PAUP3.1 with a data matrix of 29 taxa scored for 99 morphological characters (Supplementary information). Characters were scored from specimens or good photographs, not reconstruction drawings. Most parsimonious trees were identified using the heuristic search algorithm, stepwise addition, with 500 random iterations. All characters were weighted equally. Characters 15, 20, 23, 25, 32, 70 and 80 were ordered.

1. Coates, M. I. & Clack J. A. Polydactyly in the earliest known tetrapod limbs. *Nature* **347**, 66–69 (1990).
2. Clack, J. A. Earliest known tetrapod braincase and the evolution of the stapes and fenestra ovalis. *Nature* **369**, 392–394 (1994).
3. Ahlberg, P. E. *Elginerpeton pancheni* and the earliest tetrapod clade. *Nature* **373**, 420–425 (1995).
4. Lebedev, O. A. & Coates, M. I. The postcranial skeleton of the Devonian tetrapod *Tulerpeton curtum* Lebedev. *Zool. J. Linn. Soc.* **114**, 307–348 (1995).
5. Coates, M. I. The Devonian tetrapod *Acanthostega gunnari* Jarvik: postcranial anatomy, basal tetrapod interrelationships and patterns of skeletal evolution. *Trans. R. Soc. Edinb. Earth Sci.* **87**, 363–421 (1996).
6. Ahlberg, P. E., Clack, J. A. & Lukševičs, E. Rapid braincase evolution between *Panderichthys* and the earliest tetrapods. *Nature* **381**, 61–64 (1996).
7. Ahlberg, P. E. Postcranial stem tetrapod remains from the Devonian of Scat Craig, Morayshire, Scotland. *Zool. J. Linn. Soc.* **122**, 99–141 (1998).
8. Shubin, N. The evolution of paired fins and the origin of tetrapod limbs. *Evol. Biol.* **28**, 39–85 (1995).
9. Shubin, N., Tabin, C. & Carroll, S. Fossils, genes and the evolution of animal limbs. *Nature* **388**, 638–648 (1997).
10. Schultze, H.-P. Dipnoans as sarcopterygians. *J. Morphol.* **1** (Suppl.), 39–74 (1986).
11. Long, J. A. A new rhizodontiform fish from the Early Carboniferous of Victoria, Australia, with remarks on the phylogenetic position of the group. *J. Vert. Palaeontol.* **9**, 1–17 (1989).
12. Cloutier, R. & Ahlberg, P. E. in *Interrelationships of Fishes* (eds Stiassny, M. L. J., Parenti, L. R. & Johnson, G. D.) 445–479 (Academic, San Diego, 1996).
13. Johanson, Z. & Ahlberg, P. E. A complete primitive rhizodont from Australia. *Nature* **394**, 569–572 (1998).
14. Andrews, S. M. & Westoll, T. S. The postcranial skeleton of *Eusthenopteron foordi* Whiteaves. *Trans. R. Soc. Edinb.* **68**, 207–329 (1970).
15. Andrews, S. M. & Westoll, T. S. The postcranial skeleton of rhipidistian fishes excluding *Eusthenopteron*. *Trans. R. Soc. Edinb.* **68**, 391–489 (1970).
16. Jarvik, E. *Basic Structure and Evolution of Vertebrates* Vol. 1 (Academic, New York, 1980).
17. Rackoff, J. S. in *The Terrestrial Environment and the Origin of Land Vertebrates* (ed. Panchen, A. L.) 255–292 (Academic, London, 1980).
18. Rosen, D. E., Forey, P. L., Gardiner, B. G. & Patterson, C. Lungfishes, tetrapods, palaeontology, and plesiomorphy. *Bull. Am. Mus. Nat. Hist.* **167**, 159–276 (1981).
19. Holmes, E. B. Are lungfishes the sister group of tetrapods? *Biol. J. Linn. Soc.* **25**, 379–397 (1985).
20. Panchen, A. L. & Smithson, T. S. Character diagnosis, fossils and the origin of tetrapods. *Biol. Rev. Cambridge Phil. Soc.* **62**, 341–438 (1987).
21. Young, G. C., Long, J. A. & Ritchie, A. Crossopterygian fishes from the Devonian of Antarctica: systematics, relationships and biogeographic significance. *Rec. Austr. Mus.* **14** (Suppl.), 1–77 (1992).
22. Chang, M.-M. & Yu, X. Reexamination of the relationship of Middle Devonian osteolepids–fossil characters and their interpretations. *Am. Mus. Novit.* **3189**, 1–20 (1997).
23. Vorobyeva, E. I. 1977. Morphology and nature of evolution of crossopterygian fishes. *Trudy Paleontol. Inst.* **94**, 1–239 (1977).
24. Lebedev, O. A. Morphology of a new osteolepidid fish from Russia. *Bull. Mus. Nat. Hist. Nat. C* **17**, 287–341 (1995).
25. Long, J. A., Barwick, R. E. & Campbell, K. S. W. Osteology and functional morphology of the osteolepiform fish *Gogonasus andrewsae* Long, 1985, from the Upper Devonian Gogo Formation, Western Australia. *Rec. West. Aust. Mus.* **53** (Suppl.), 1–89 (1997).
26. Andrews, S. M. Rhizodont crossopterygian fish from the Dinantian of Foulden, Berwickshire, Scotland, with a re-evaluation of this group. *Trans. R. Soc. Edinb. Earth Sci.* **76**, 67–95 (1985).
27. Ahlberg, P. E. & Johanson, Z. Second tristichopterid (Sarcopterygii, Osteolepiformes) from the Upper Devonian of Canowindra, New South Wales, Australia, and phylogeny of the Tristichopteridae. *J. Vert. Palaeontol.* **17**, 653–673 (1997).
28. Vorobyeva, E. I. & Schultze, H.-P. in *Origins of the Higher Groups of Tetrapods: Controversy and Consensus* (eds Schultze, H.-P. & Trueb, L.) 68–109 (Cornell Univ., Ithaca, 1991).
29. Johanson, Z. & Ahlberg, P. E. New tristichopterid (Osteolepiformes: Sarcopterygii) from the Mandagery Sandstone (Famennian) near Canowindra, N. S. W., Australia. *Trans. R. Soc. Edinb. Earth Sci.* **88**, 39–68 (1997).
30. Chang, M.-M. & Min, Z. A new Middle Devonian osteolepid from Qujing, Yunnan. *Mem. Ass. Australasian Palaeontol.* **15**, 183–198 (1993).

Weak trophic interactions and the balance of nature

Kevin McCann, Alan Hastings & Gary R. Huxel

Department of Environmental Sciences and Policy, University of California, Davis, California 95616, USA

Ecological models show that complexity usually destabilizes food webs[1,2], predicting that food webs should not amass the large numbers of interacting species that are in fact found in nature[3–5]. Here, using nonlinear models, we study the influence of interaction strength (likelihood of consumption of one species by another) on food-web dynamics away from equilibrium. Consistent with previous suggestions[1,6], our results show that weak to intermediate strength links are important in promoting community persistence and stability. Weak links act to dampen oscillations between consumers and resources. This tends to maintain population densities further away from zero, decreasing the statistical chance that a population will become extinct (lower population densities are more prone to such chances). Data on interaction strengths in natural food webs[7–11] indicate that food-web interaction strengths are indeed characterized by many weak interactions and a few strong interactions.

Here we combine formally the influence of interaction strength with modern food-web data and models, uniting verbal arguments[12–16] with the rigorous formulations of May[1,2]. Our analysis differs from May's contributions in five important ways. First, we use a measure of interaction strength that is based upon empirical estimates of per capita interaction strength; second, we assume that communities can display nonequilibrium dynamics; third, we construct complexity as simple food webs (after ref. 17) in a manner consistent with patterns found in nature[14–16]; fourth, we use biomass as the model currency; and fifth, we use consumption rates that become saturated as resource density increases (that is, we use type II functional responses). We describe our model and define terms in Box 1.

It is well known that the model food chain (Fig. 1a) exhibits several behaviours (such as stable equilibria, cycles, chaos and multiple attractors)[18–20]. In a simplified sense, the food chain is best understood by considering it as two coupled consumer–resource subsystems: a consumer–resource interaction (that is, the interaction between C_1 and R in Equation set (1), box 1) and the top-predator–consumer interaction (that is, the interaction between P and C_1 of Equation set (1)). For example, if the food chain is constructed from two strong consumer–resource interactions (that is, both subsystems produce cyclic behaviour) then the food chain behaviour becomes quite complex and variable[18–20]. In this case, the food chain can be seen two coupled oscillators whose dynamics depend on whether the frequencies of these oscillators are commensurate (producing cyclic dynamics) or incommensurate (producing quasi-periodic or chaotic dynamics).

Two corollaries follow from these statements: first, stabilizing all the underlying oscillators eliminates the occurrence of cyclic or chaotic dynamics in the full system; and second, reducing the amplitude of the underlying oscillators reduces the amplitude of the dynamics of the full system. Thus we predict that inhibiting strong consumer–resource interactions within a food web promotes persistence in food webs.

We study below how interaction strength influences oscillatory subsystems of more complicated food webs (Fig. 1b–f). We show that weak interactions can act to inhibit potentially oscillatory subsystems through the following three naturally occurring mechanisms.

In the apparent competition mechanism, apparent competition among resource species occurs when a consumer preys upon multiple resources. In this case, a consumer can inhibit a potentially oscillatory consumer–resource interaction when it trades off preference for one resource (that is, that resource involved in the potentially oscillatory consumer–resource interaction) in order to feed on a second resource. This effectively reduces the efficiency at which the consumer attacks the first resource.

In the exploitative competition mechanism, two consumers compete for the same resource. In this case, the addition of a second competitor reduces the growth rate of the shared resource item (from the perspective of the first consumer) and, therefore, can inhibit a potentially oscillatory consumer–resource interaction involving the first consumer.

In the food-chain-predation mechanism, food-chain predation occurs when a top predator feeds on an intermediate consumer which feeds on a resource. The top predator can inhibit the growth rate of its resource (the intermediate consumer) and, therefore, inhibit the intermediate-consumer–resource trophic interaction. The top predator reduces the intermediate consumer's attack rate on the resource item.

At the heart of these mechanisms is the concept that a stable consumer–resource interaction is required to dampen the dynamic

---

Box 1 The food-web model

We used the following model:

$$\frac{dR}{dt} = R\left(1 - \frac{R}{K}\right) - \frac{\Omega_{C_1R}x_{C_1}y_{C_1}C_1R}{\Omega_{C_1R}R + (1 - \Omega_{C_1R})C_2 + R_0} - \frac{\Omega_{C_2R}x_{C_2}y_{C_2}C_2R}{R + R_0}$$

$$\frac{dC_1}{dt} = -x_{C_1}C_1\left(1 - \frac{\Omega_{C_1R}y_{C_1}R + (1 - \Omega_{C_1R})y_{C_1}C_2}{\Omega_{C_1R}R + (1 - \Omega_{C_1R})C_2 + R_0}\right)$$
$$- \frac{\Omega_{PC_1}x_P y_P C_1 P}{\Omega_{PC_1}C_1 + (1 - \Omega_{PC_1})C_2 + C_0}$$

$$\frac{dC_2}{dt} = -x_{C_2}C_2\left(1 - \frac{\Omega_{C_2R}y_{C_2}R}{R + R_0}\right) - \frac{(1 - \Omega_{PC_1})x_P y_P C_2 P}{\Omega_{PC_1}C_1 + (1 - \Omega_{PC_1})C_2 + C_0}$$
$$- \frac{(1 - \Omega_{CR_1})x_{C_1}y_{C_1}C_1C_2}{\Omega_{C_1R}R + (1 - \Omega_{C_1R})C_2 + R_0} \quad (1)$$

$$\frac{dP}{dt} + -x_P P\left(1 - \frac{\Omega_{PC_1}y_P C_1 + (1 - \Omega_{PC_1})y_P C_2}{\Omega_{PC_1}C_1 + (1 - \Omega_{PC_1})C_2 + C_0}\right)$$

where R is resource density, C_1 is the density of the first consumer species, C_2 is density of the second consumer species and P is density of the top predator. The parameters correspond to a bioenergetic interpretation of the Rosenzweig-MacArthur model[28], in which K is the resource carrying capacity; R_0 and C_0 are the half-saturation densities of the resource, R, and consumer, C_1, respectively; x_i is the mass-specific metabolic rate of species i, measured relative to the production-to-biomass ratio of the resource population; y_i is a measure of ingestion rate per unit metabolic rate of species i; and Ω_{ij} is a fraction indicating the preference of species i for consuming resource species j (ref. 29). Through choice of preference parameters (Ω_{ij}), this model can be made to represent the simple food-chain model (Fig. 1a), exploitative competition (Fig. 1b), apparent competition (Fig. 1c) and intraguild predation (Fig. 1d).

Equation set (1) relies on the assumption of saturating consumption rate, $F_k(i,j)$, such that a consumer, k, captures resources i and j according to the following type II multispecies functional response[29].

$$F_k(i,j) = F_k(i) + F_k(j) = \frac{\Omega_{ki}x_k y_k i}{\Omega_{ki}i + (1 - \Omega_{ki})j + i_0} + \frac{(1 - \Omega_{ki})x_k y_k j}{\Omega_{ki}i + (1 - \Omega_{ki})j + i_0}$$
$$= \frac{\Omega_{ki}x_k y_k i + (1 - \Omega_{ki})x_k y_k j}{\Omega_{ki}i + (1 - \Omega_{ki})j + i_0} \quad (2)$$

Equation (2) indicates the flow of biomass from resource i and j to consumer k, so it is natural to define the per capital interaction strength, α_{ki}, of resource species i on consumer species k as:

$$\alpha_{ki} = \frac{F_k(i)}{i} = \frac{\Omega_{ki}x_k y_k}{\Omega_{ki}i + (1 - \Omega_{ki})j + i_0} \quad (3)$$

We define the interaction strength, I_{ki}, as the maximum per capita interaction strength of resource species j on the consumer species i. As αki, has its maximum when resource densities approach zero (that is, when all consumer i's resources approach 0), then the interaction strength is:

$$I_{ki} = \frac{\Omega_{ki}x_k y_k}{i_0} \quad (4)$$

If we assume a type I functional response ($F(j) = \Omega_{ki}x_k y_k j$) then Equation (3) is the standard form for the per capita interaction strength[7,9]. Similarly, the interaction strength of consumer species i on resource species j can be defined to be equal in magnitude to Equation (3) and Equation (4) but opposite in sign ($\alpha_{ij} = -\alpha_i$; $I_{ij} = -I_{ji}$).

We now estimate[28] the maximum biologically plausible value of interaction strength I_{ij} in system (1). If we know average adult body sizes and the metabolic type (endotherm, vertebrate ectotherm or invertebrate) of species i, we can then estimate biologically plausible values for x_i and for the maximum value of y_i ($y_{max,i}$; this occurs when ingestion, y_i, is limited by an animal's physiological capacity). Hence, given i's preference for species j and the half-saturation density, j_0, we can estimate the interaction strength, which we call the interaction scope as it defines the maximum biologically plausible upper limit to I_{ij}. In nature it is likely that consumers operate at a maximum that is some fraction of the interaction scope (at the realizable interaction scope) because of limitation by ecological factors[28]. Nevertheless, the estimates for interaction scope allow us to make some predictions concerning food-web complexity and metabolic type.

Assume that any consuming species involved in a single consumer-resource interaction is operating at its realizable interaction scope (that is, at is realizable maximum rate of ingestion). Hence, as species i is operating at its realizable interaction scope, while consuming a single species j (that is, $\Omega_{ij} = 1$), then choosing to consume another resource item requires that species i trade off some of its preference for consuming species j ($\Omega_{ij} < 1$), so the preference for the new resource is $1 - \Omega_{ij}$ (ref. 29). This allows us to compare complexity–stability arguments in a consistent manner.

behaviour of a potentially strong interaction (and, hence, a potentially oscillatory interaction). Consistent with the theory of consumer–resource interactions, reduction in growth rates of the resource and reduction in attack rates by the consumer tend to stabilize a consumer–resource interaction[21].

We now blend more food-web structure into the simple food-chain model (Fig. 1a), enabling us to study the dynamic implications of naturally occurring food-web structures[4,14–16]. Looking at exploitative competition[22] (Fig. 1b), apparent competition[23] (Fig. 1c), and intraguild predation[24] in which consumer 1 feeds on both the basal resource and a second consumer (Fig. 1d), we discuss how the three inhibiting mechanisms naturally arise and work to stabilize food-web dynamics. We then discuss how these mechanisms also arose in previous studies in which it was found that weak amounts of omnivory[22,25,26] (Fig. 1e) and external (allochthonous) inputs[4,27] (Fig. 1f) can enhance food-web stability.

To study exploitative competition, we began with parameters for a biologically plausible example of persistent chaotic dynamics for a three-species food chain (Ω_{ij} values = 1; $x_{C_1} = 0.40$; $y_{C_1} = 2.009$; $x_P = 0.08$; $y_P = 5.0$; $C_0 = 0.50$; and $R_0 = 0.16129$; see Box 1 for definitions)[19]. Figure 1b shows the addition to this chain of a second intermediate consumer (C_2), which interacts with the basal resource, R, with a strength governed by the parameter Ω_{C_2R}. In this case, Equation set (1) has the following extra parameters: $x_{C_2} = 0.20$; $y_{C_2} = 3.50$; $R_{02} = 0.90$. We chose the new consumer, C_2, to be competitively inferior to C_1, so its ability to persist is mediated by the selective predation of the top predator, P, on C_1. Figure 2a depicts the local minima and maxima attained for the top predator densities, P, in solutions to Equation set (1) across a range of C_2–R interaction strengths relative to C_1–R interaction strengths (that is, I_{C_2R}/I_{C_1R}). Figure 2a also shows food-web diagrams that depict the change in food-web structure as the relative interaction strength changes value.

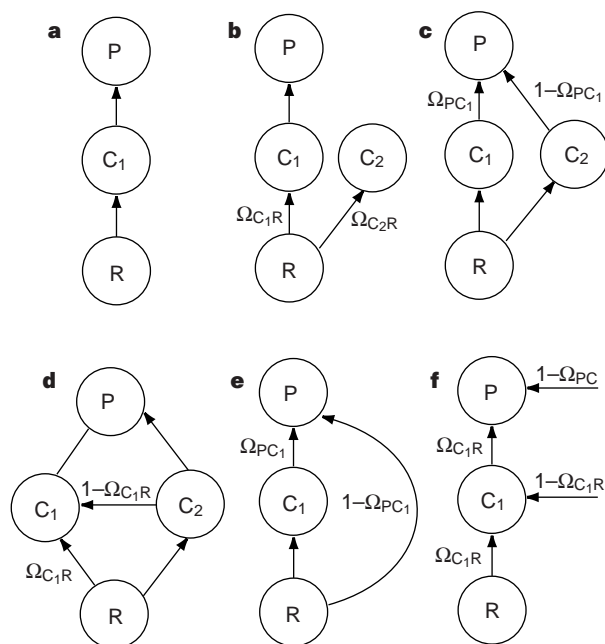In this scenario we expect the exploitative competition mechan-

ism to inhibit the oscillating C_1–R subsystem. It does exactly this when C_2 can invade ($I_{C_2R}/I_{C_1R} \approx 0.102$). Below this value the original food chain (P–C_1–R) remains intact and continues to exhibit chaotic dynamics (shown by the thick set of points from 0.50 to 0.57 in Fig. 2a). However, when C_2 can invade, the dynamics immediately begin to take on a much simpler periodic signal that tends further away from zero (0.102–0.125). Equation set (1) does not reach an equilibrium solution over this range, as the P–C_1 oscillator remains intact—none of the mechanisms is operating to inhibit this oscillatory component.

When the relative interaction strength increases beyond 0.125, the attractor begins to become less bounded again and eventually undergoes a period-doubling cascade to a more complex dynamical regime above $I_{C_2R}/I_{C_1R} \approx 0.15$. The new C_2–R interaction has become too strong (and therefore oscillatory) and no longer dampens the system; it contributes to the chaos by adding a third oscillating subsystem to the food web.

To study apparent competition, we began with the same parameters as above except that we let $I_{C_2R}/I_{C_1R} \approx 0.154$ (that is, $\Omega_{C_2R} = 0.98$). This returns us to a complex oscillatory food-web dynamic (Fig. 2a); however, in this case, we have three oscillatory subsystems (P–C_1, C_1–R, and C_2–R). We now construct a link between the top predator, P, and the second intermediate consumer, C_2 (Fig. 1c), by allowing Ω_{PC_1} to be <1, creating apparent competition between the two intermediate consumers.

Figure 2b shows the local minima and maxima for the top predator, P, in solutions to Equation set (1) across a range of strengths of the P–C_2 interaction relative to strengths of the P–C_1 interaction (I_{PC_2}/I_{PC_1}). We expect the apparent competition mechanism to inhibit the C_2–R and C_1–R oscillators. As relative interaction strength increases from zero, it immediately causes a period-doubling reversal, forcing simpler, more bounded, limit cycle dynamics for $I_{PC_2}/I_{PC_1} \approx 0.03–0.10$ and stable equilibrium dynamics for $I_{PC_2}/I_{PC_1} \approx 0.10–0.12$. As before, increasing the strength of the interaction further eventually destabilizes the system. Despite the complexity of this system, which includes multiple attractors and numerous bifurcations, qualitatively the result remains: relatively weak links simplify and bound the dynamics of food webs.

We now construct a link such that C_1 can feed on C_2 (Fig. 1d), creating intraguild predation within the food web. The parameters are the same as in the previous case, with $I_{PC_2}/I_{PC_1} \approx 0.01$; (that is, $\Omega_{PC_1} = 0.99$) so that we start off with a complex oscillatory dynamic (we have three oscillators in the food web again). Figure 2c shows the local minima and maxima for the top predator, P, in solutions to Equation set (1) across a range of the relative interaction strength $I_{C_1C_2}/I_{C_1R}$. Here, we expect the apparent competition mechanism to inhibit the C_1–R subsystem and we expect the food-chain mechanism to inhibit the C_2–R subsystem. As a result of having two inhibitors and three potential oscillators, the dynamics never reach a locally stable equilibrium; they attain a well-bounded limit cycle solution (driven by the remaining oscillating P–C_1 subsystem) for most $I_{C_1C_2}/I_{C_1R}$ values above 0.05.

In two of the cases above, weak links failed to beget stable local equilibria with all species present—at best we get well-bounded limit cycle solutions. This is because, in these two cases, there is not an inhibiting mechanism for each potential oscillator. This is largely a result of our choice of starting with chaotic dynamics and adding only one additional food-web interaction at a time: our analysis biases our results to have fewer inhibitors than oscillators. Finally we show that adding another, appropriately directed, inhibiting mechanism to such a situation allows for rapid local stabilization to an equilibrium solution. Figure 2d depicts solutions to system 1 when we start off with $I_{C_2R}/IC_1R = 0.11$ (Fig. 2a). Thus, we are starting off with one oscillating subsystem (the P–C_1 subsystem). After adding the apparent competition mechanism, which inhibits the P–C_1 subsystem, we rapidly get a locally stable solution for weak relative interaction strengths (by $I_{PC_2}/I_{PC_1} \approx 0.040$ in Fig. 2d).
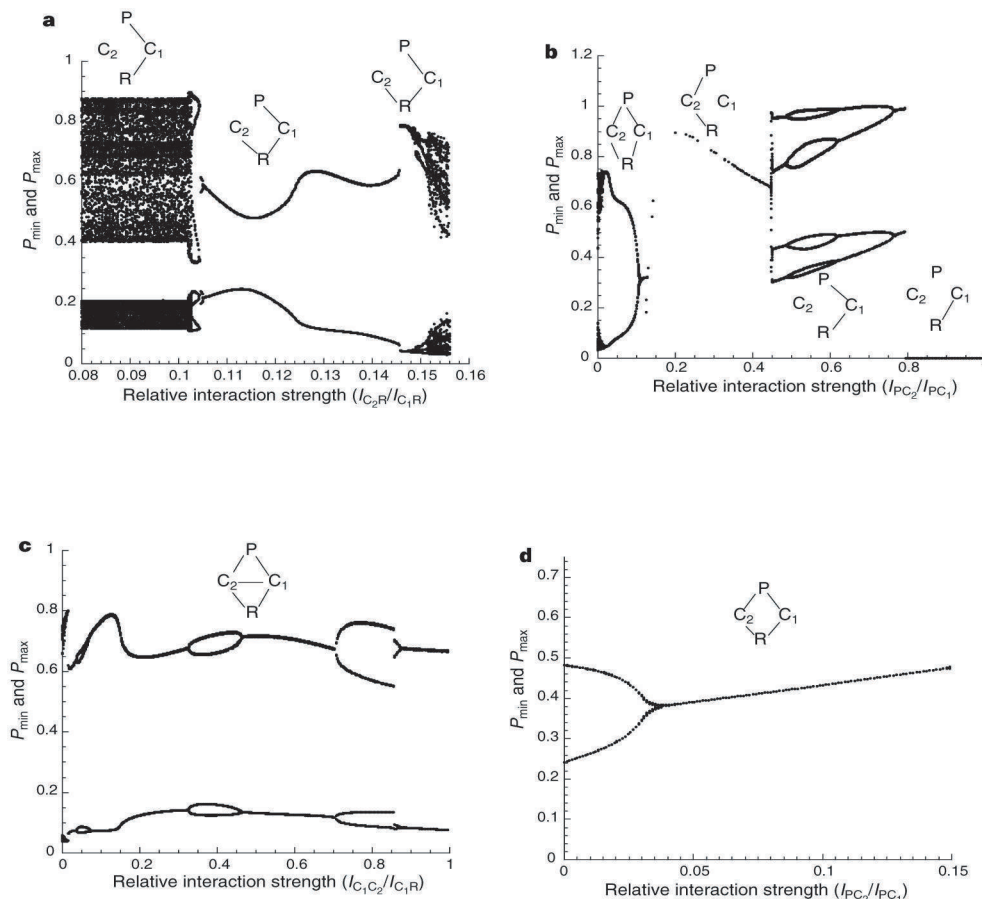

Figure 1 The six food-web configurations studied are: **a**, a simple food chain, **b**, a food web with multiple intermediate consumers (exploitative competition), **c**, a food web with the top predator feeding on two intermediate consumers (apparent competition), **d**, a food web with consumer 1 feeding on the basal resource and on the second consumer (intraguild predation), **e**, a food chain including omnivory, and **f**, a food chain with external inputs. R denotes the basal resource species; C_1 and C_2 denote intermediate consumer species 1 and 2; and P denotes the top predator (Box 1).

Figure 2 The local minima and maxima for top predator density, **P**, attained in the attracting solutions for a range of relative interaction strengths. Food-web configurations are given as a function of the relative interaction strengths. Food-web configurations are given as a function of the relative interaction strength. Whenever the configuration lacks an explicit link between a species and the rest of the connected web this implies that the species cannot persist. a, Exploitative competition. b, Apparent competition. c, Intraguild predation. d, The configuration used in b, starting with a limit cycle solution ($I_{C_2R}=I_{C_1R} ? 0.62$).

Using a model formulation similar to system 1, two groups[26,27] have shown that weak amounts of omnivory (Fig. 1e) and allochthonous inputs (Fig. 1f) bound the magnitude of the oscillations in $P–C_1–R$ densities further away from zero. In both cases, chaotic dynamics collapsed through period-doubling reversals (that is, the periodicity of solutions reduced from n to $n/2$ to $n/4$ etc.) into well-bounded cyclic or stable dynamics under weak to moderate amounts of omnivory and allochthonous inputs. Both results can be explained with our proposed mechanisms.

Several testable predictions for food webs result from our study. First, if a relatively weak interaction exists for each strong consumer–resource interaction, then the food web should be stabilized relative to the oscillatory subsystems (that is, the food web should be less oscillatory). Second, if food webs have many weak interactions, then, at least form a deterministic viewpoint, chaotic dynamics are unlikely. Third, generalist-dominated food webs should exhibit less variable dynamics than specialist-dominated food webs. Fourth, depauperate food webs should tend to be more oscillatory than reticulate food webs as depauperate food web species tend to have larger average interaction strengths, thus promoting the dominance of a few strong (oscillatory) interactions. Finally, if we assume the realizable interaction scope is proportional to interaction scope, then given all else equal, endotherms ($y_{maxi} ? 1.60$) and vertebrate ectotherms ($y_{maxi} ? 3.90$) are more likely to be stabilized by weak food web links than invertebrates as invertebrates have a greater interaction scope (since $y_{maxi} ? 19.4$) and thus greater potential to maintain a larger number of strong consumer–resource interactions. A larger number of strong consumer-resource interactions requires a greater number of weak interactions to inhibit oscillatory subsystems. It follows, given topologically identical food webs, that invertebrate-dominated communities are more likely to have the most oscillatory dynamics. Our overall conclusion is that knowledge of interaction strength in study of food webs is vital. Although few quantitative field estimates of interaction strength are available, early data unequivocally indicate that distributions of interaction strength are strongly skewed towards weak interactions[7–11]. It seems, then, that weak interactions may be the glue that binds natural communities together. □

1. May, R. M. Stability in multi-species community models. *Math. Biosci.* **12**, 59–79 (1971).
2. May, R. M. *Stability and Complexity in Model Ecosystems* (Princeton Univ. Press, Princeton, 1973).
3. Winemiller, K. O. Spatial and temporal variation in tropical fish trophic networks. *Ecol. Monogr.* **60**, 331–367 (1990).
4. Polis, G. A. Complex trophic interactions in deserts: an empirical critique of food web theory. *Am. Nat.* **138**, 123–155 (1991).
5. Lavigne, D. M. in *Studies of High Latitude Homeotherms in Cold Ocean Systems* (ed. Montevecchi, W. A.) 95–102 (Canadian Wildlife Service Occasional Paper, Ottawa, Canada, 1995).
6. Gardner, M. & Ashby, W. R. Connectance of large dynamical (cybernetic) systems: critical value for stability. *Nature* **228**, 784 (1970).
7. Paine, R. T. Food-web analysis through field measurement of per capita interaction strength. *Nature* **355**, 73–75 (1992).
8. Fagan, W. F. & Hurd, L. E. Hatch density variation of a generalist athropod predator: population consequences and community impact. *Ecology* **75**, 2022–2032 (1994).
9. Wootton, J. T. Estimates and test of per capita interaction strength: diet, abundance, and impact of intertidally foraging birds. *Ecol. Monogr.* **67**, 45–64 (1997).
10. Goldwasser, L. & Roughgarden, J. Construction and analysis of a large caribbean food web. *Ecology* **74**, 1216–1233 (1993).
11. Rafaeli, D. G. & Hall, S. J. in *Food Webs: Integration of Patterns & Dynamics* (eds Polis, G. A. & Winemiller, K. O.) 185–191 (Chapman & Hall, New York, 1996).

12. MacArthur, R. H. Fluctuations of animal populations and a measure of community stability. *Ecology* **36**, 533–536 (1955).

13. Elton, C. S. *Ecology of Invasions by Animals and Plants* (Chapman & Hall, London, 1958).

14. Strong, D. Are trophic cascades all wet? Differentiation and donor-control in speciose ecosystems. *Ecology* **73**, 747–754 (1992).

15. Polis, G. A. Food webs, trophic cascades and community structure. *Aust. J. Ecol.* **19**, 121–136 (1994).

16. Polis, G. A. & Strong, D. Food web complexity and community dynamics. *Am. Nat.* **147**, 813–846 (1996).

17. Holt, R. D. in *Multitrophic Interactions* (eds Begon, M., Gange, A. & Brown, V.) 333–350 (Chapman & Hall, London, 1996).

18. Hastings, A. & Powell, T. Chaos in a three species food chain model. *Ecology* **72**, 896–903 (1991).

19. McCann, K. & Yodzis, P. Biological conditions for chaos in a three-species food chain. *Ecology* **75**, 561–564 (1995).

20. De Feo, O. & Rinaldi, S. Singular homoclinic bifurcations in tritrophic food chains. *Math. Biosci.* **148**, 7–20 (1998).

21. Rosenzweig, M. & McArthur, R. H. Graphical representation and stability conditions of predator-prey interactions. *Am. Nat.* **107**, 275–294 (1963).

22. Diehl, S. Relative consumer sizes and the strengths of direct and indirect interactions in omnivorous feeding relationships. *Oikos* **68**, 151–157 (1993).

23. Holt, R. D. Predation, apparent competition, and the structure of prey communities. *Theor. Popul. Biol.* **12**, 197–229 (1977).

24. Polis, G. A. & Holt, R. D. Intraguild predation: the dynamics of complex trophic interactions. *Tree* **7**, 151–155 (1992).

25. Fagan, W. F. Omnivory as a stabilizing feature of natural communities. *Am. Nat.* **150**, 554–567 (1997).

26. McCann, K. & Hastings, A. Re-evaluating the omnivory-stability relationship in food webs. *Proc. R. Soc. Lond. B* **264**, 1249–1254 (1997).

27. Huxel, G. & McCann, K. Food web stability: the influence of trophic flows across habitats. *Am. Nat.* **152**, 460–469 (1998).

28. Yodzis, P. & Innes, S. Body-size and consumer-resource dynamics. *Am. Nat.* **139**, 1151–1175 (1992).

29. Chesson, J. The estimation and analysis of preference and its relationship to foraging models. *Ecology* **64**, 1297–1304 (1983).

A jitter after-effect reveals motion-based stabilization of vision

Ikuya Murakami & Patrick Cavanagh

Department of Psychology, Harvard University, 33 Kirkland Street, Cambridge, Massachusetts 02138, USA

A shaky hand holding a video camera invariably turns a treasured moment into an annoying, jittery momento. More recent consumer cameras thoughtfully offer stabilization mechanisms to compensate for our unsteady grip. Our eyes face a similar challenge in that they are constantly making small movements even when we try to maintain a fixed gaze[1]. What should be substantial, distracting jitter passes completely unseen. Position changes from large eye movements (saccades) seem to be corrected on the basis of extraretinal signals such as the motor commands sent to the eye muscle[2–5], and the resulting motion responses seem to be simply switched off[6,7]. But this approach is impracticable for incessant, small displacements, and here we describe a novel visual illusion that reveals a compensation mechanism based on visual motion signals. Observers were adapted to a patch of dynamic random noise and then viewed a larger pattern of static random noise. The static noise in the unadapted regions then appeared to 'jitter' coherently in random directions. Several observations indicate that this visual jitter directly reflects fixational eye movements. We propose a model that accounts for this illusion as well as the stability of the visual world during small and/or slow eye movements such as fixational drift, smooth pursuit and low-amplitude mechanical vibrations of the eyes.

The experimental setting required for this illusion has three conditions: (1) adaptation to dynamic random noise in a local region (referred to as the adapted area) for at least several seconds; (2) a successive test with static random noise in the adapted area plus static noise in a region somewhere near the adapted area (referred to as the unadapted area); and (3) maintained fixation throughout these two periods. During the adaptation period, static noise is typically presented in the unadapted region (Fig. 1a), although leaving it blank does not change the outcome (Fig. 1b). After adaptation, static noise presented in the unadapted region seems to jitter rigidly (all dots moving together) in random directions for several seconds. In contrast, the static noise in the
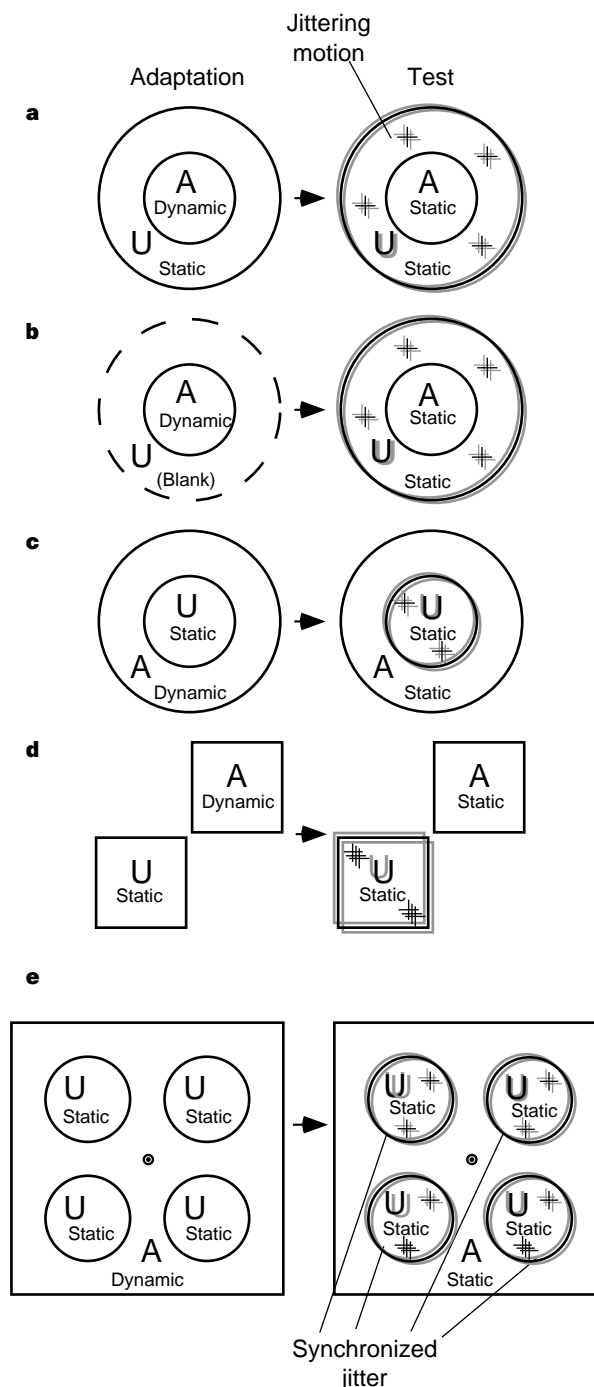

Figure 1 A schematic view of the stimulus configuration and perception. **a–e**, The various configurations used in these experiments and their outcomes. A fixation point is typically provided at the centre of the stimulus, but the illusion occurs for peripheral viewing as well. A and U stand for adapted and unadapted (static or blank) regions, respectively. The blur of circles and crosses in the test stimuli depicts the visual jitter schematically. See http://visionlab.harvard.edu/ for demonstrations.